Increasing hybrid PV/wind/diesel generator power output with increased PV module efficiency.

L O Idoko[1], O Anaya-Lara[1] and A Attya[2]
[1] Department of EEE, University of Strathclyde. Glasgow, UK.
[2] School of Computing & Engineering, University of Huddersfield, UK.
E-mail: oneplus8@yahoo.com

Abstract. This research work focuses on increasing the power output of a hybrid energy system by giving a boost to the energy supplied from the PV module. It embraces the cooling of the PV module using a multi-concept cooling technique. An experiment was set up to reduce the surface temperature of the PV module to 20°C in order to increase its efficiency and hence power output. The experiment was performed using two 250 watts PV modules, water spraying was carried out on one of the modules which, was also attached with an Aluminium heat sink at the rear, while the other module was mounted without any form of cooling. The modelling of the hybrid energy system was done using MATLAB Simulink. An equation for PV module power output was used with a derating factor of 95% and the result of the experiment shows that power output of 262.4 watts is achievable, and the simulation result shows an increase in the power contributed by the module.

1. Introduction

The growth of any developing nation depends largely on the accessibility of adequate Power, as the availability of adequate power is a necessity, for an appreciable economic and technological development to be achieved.

Sources of energy supply from natural resources such as wind and sunlight provides a clean alternative source of power in locations which experiences high sunshine and high wind speed and as a result, energy from renewable sources can compete favourably with energy generation from fossil fuel, which usually introduce pollution to the environment [1].

The PV module is a good source of energy in Nigeria and other parts of the world, which experiences long periods of sunshine. In locations where long period of sunshine hours is experienced during the day, the excess sunlight is not fully utilized due to the effect of temperature on the PV module.

As the intensity of the sun increases, the temperature of the module surface also increases. Temperatures about 25°C causes the power output from the solar panel to reduce. Imagine a situation where the temperature of the surface of the module increases above 45°C, a lot of the incident radiation is converted to electricity and heat energy.

The energy converted to heat energy is wasted in the process, hence, the power output generated by the PV module reduces as the temperature of the module surface increases. In order to make the module more efficient, cooling of the surface of a PV module is a necessity [2]. A recent research, [3] shows that when you place a PV module under sunlight, only about 31% of the energy from the sun is converted to useful energy, the remaining percentage is converted to heat energy which usually causes the temperature of the module to increase and this gives rise to the following challenges:

- There is a reduction in the electricity produced by the module
- The increase in the module temperature due to the energy wasted as heat can damage the material used to fabricate the module.

- The conversion efficiency of the PV module also reduces.

In order for us to maximize the use of the available energy from the sun to generate electricity, cooling of the PV module is a necessity.

1.1. Multi-concept cooling technique

This research work embraces a multi-concept cooling technique to help reduce the energy wasted as heat energy when a PV module is placed under sunlight. The aim is to extract the excess energy, which causes the temperature of the PV module surface to rise to a level, where the power output reduces due to a reduction in the conversion efficiency of the module. The concept involves:

- Cooling the surface of the PV module to a temperature of 20°C using water
- Attaching aluminium heat sink at the rear of the PV module.
- Mounting of the module at a considerable height above the ground to enhance air-cooling.

Cooling of the module surface with water helps to reduce the temperature of the module surface considerably; this helps to increase the conversion efficiency of the PV module. Conversely, the aluminium heat sink attached to the rear of the module serves two functions: it helps to extract heat from the rear of the module and, it also helps the module to maintain a uniform temperature.

1.2. New features and advantages of proposed method.

The new features of the proposed method include the followings: cooling of the module is achieved using multi-concept cooling technique, ice blocks is added to the cooling water to reduce its temperature and cooling is applied at the surface as well as the rear of the module.

Conversely, the main advantages of this method are as follows: maintaining the temperature of the module surface at 20°C ensures the module yields steady increase in power output, at an irradiance of 1000w/m² , more power than the module rated capacity is achieved and in the absence of any of the three concepts of cooling involved, a certain amount of cooling can be achieved.

1.3. The efficiency of PV module

The efficiency, η of a PV module is generally defined as in [2], as the ratio of the energy produced by the module to the energy obtained from the sun. It can be represented mathematically as equation (1)

$$\eta = E_{pd} / E_{ob} = P_{\max} / E.A \tag{1}$$

Where P_{max} represents the maximum power obtained from the module, the solar irradiance at STC in W/m2 is represented by E, while A represents the module surface area (m²).

E_{pd} and E_{ob} represent the energy produced by the module and the energy obtained from the sun respectively. The PV module efficiency can also be represented as equation (2).

$$\eta_m = \eta_{rT}[1 - \beta(T_m - T_{rT})] \tag{2}$$

Where η_m is the module efficiency, η_{rT} represents the module efficiency at 25°C, T_m is the module temperature, β is the temperature coefficient of power and T_{rT} represents module reference temperature.

1.4. The effect of Temperature on PV module

In order to account for the effect of temperature on a PV module, the PV module power output as in [4] is expressed using equation (3).

$$P_{pv} = Y_{pv}.f_{pv}(G_T / G_{T,STC})[1 + \alpha_p(T_C - T_{C,STC})] \tag{3}$$

Where

f_{pv} represents the derating factor (%) of the PV module,

Y_{pv} represents the PV array rated capacity at STC ((KW)

G_T represents the amount of solar radiation incident on the PV array (KW/m²)

$G_{T,STC}$ represents the amount of incident radiation at STC (1Km/m²)

α_p represents the temperature coefficient of power (%/°C)

T_C represents the temperature of the PV cell (°C)

$T_{C,STC}$ represents temperature of the PV cell under standard test conditions (25°C)

1.5. Research location

The experiment carried out in order to increase the efficiency of the PV module was performed in Sokoto state, in northern Nigeria located within Latitude 13.1274 and Longitude 5.2046, an area which, experiences a long period of intense sunlight. The sunshine hours data for Sokoto, Sokoto State, Nigeria is as shown in Figure 1.
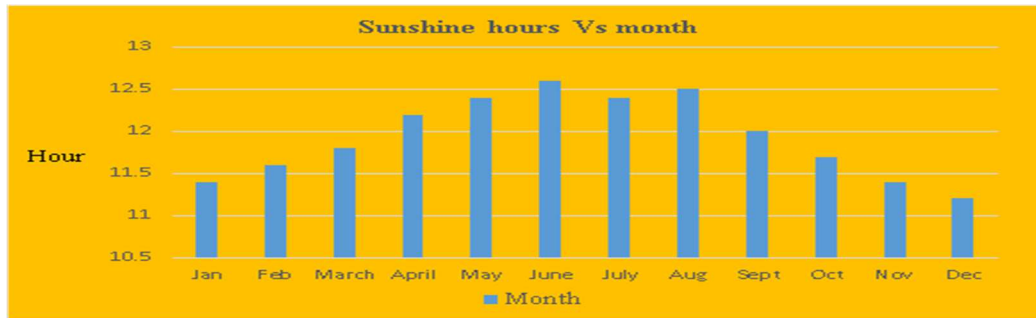
Figure 1. Sunshine hours in Sokoto in the 2016.

The aim of the experiment is to improve the efficiency of the PV module and in the process, increase the amount of energy contributed to the hybrid energy system by the PV.

2. Materials

The experiment was carried out successfully using the following devices as shown in Table 1

Table 1. Devices used for the experiment.

Device	Quantity
250 watts PV module	2
Aluminium heat sink	1
10 litres water spraying can	1
AL 300 data logger (6-channels)	1
Digital Multimeter	4
Infrared thermometer	1
Meteon Pyranometer and display unit	1
Long nose plier	1
Multipurpose plier	1
A set of spanners	1
Measuring tape	1

The experiment requires the use of both 250 watts, as one of the modules was mounted without an attached aluminium heat while the other has an attached aluminium heat sink. The Aluminium heat is fabricated using an Aluminium sheet with a dimension of 154 cm x 93cm x 0.1cm on which several Aluminium fins with fin base of 2.4cm each, were mounted.

3. Method

The experiment was setup as shown in Figure 2. One of the module is mounted without any form of attachment while the other module is mounted with the heat sink attached to the rear of the module. In order to create room for air-cooling, both modules were mounted at a height of 137cm above the ground level, the Al 300 six-channel data logger, Pyranometer, variable resistors and digital Multimeters were all mounted properly as shown in Figure 2 and readings were taken.

Figure 2. Project setup

The function of the Al heat sink attached to the rear of one the module, is to extract heat from the module and keep the temperature uniform while, cooling of the surface of the PV module was carried out by spraying the surface of the PV module with water.

Ice blocks were introduced into the cooling water to reduce the temperature of the cooling water, spraying of the module was done with the cold water and a module surface temperature of about 20°C was achieved. Spraying of the module was carried out as shown in Figure 3.

Figure 3. Spraying of PV module with cold water.

The results of the experiment are as shown in Table 2, the power output of the PV module at a derating factor of 95% was calculated using equation (3). The calculation was carried out for the module without aluminium heat sink and cooling, the module with Aluminium heat sink + water-cooling, and finally it was used to compute the power output of the module when the module surface temperature was reduced to 20°C

Using a derating factor of 95% to comply with the PV manufacturer's data sheet which, has a power tolerance of ± 5% gives Table 2

Table 2. Module power output at a derating factor of 95%.

Time	Ambient temp (°C)	Panel without Al heat sink, surface temp (°C)	Module + Al heat sink & water-cooling surface temp (°C)	Solar radiation (Wm-2)	Module without Al heat sink power output (w) at f_{pv} = 95%	Module + Al heat sink & water-cooling, power output (w) at f_{pv} = 95%	Module + Al heat sink & water-cooling of module surface to 20°C power output (w) at f_{pv} = 95%
09:00	36	40.3	40.3	407	90.16	90.16	
09:15	36.9	46.7	46.3	558	119.9	120.1	
09:30	36.8	45	44	736	159.4	160.2	
09:45	38	50.1	49.5	779	164.6	165.1	
10:00	40	55	53.4	789	162.7	164	
10:15	40.9	53.3	51	826	171.7	173.7	
10:30	43.3	54.1	52	897	185.8	187.7	
10:45	43.9	56.8	54.5	932	190.4	192.6	
11:00	44	58.6	53	955	193.3	198.9	
11:15	46	59.4	54.2	960	193.5	198.7	
11:30	47.6	61	54	1017	203.3	210.7	
11:45	47.9	61.2	54.3	1019	203.5	210.8	
12:00	49	63	55.9	1021	201.9	209.5	
12:15	47.7	60	57.2	1072	215.4	218.5	
12:30	43.6	56.6	55	1097	224.3	226.1	
12:45	49.5	64.1	39	1081	212.6	240.9	262.4
13:00	45.3	54	50	1126	233.3	238	
13:15	46.7	55.2	51	1085	223.4	228.2	
13:30	41.1	51.4	48	1073	225.2	229	
13:45	41.1	51.5	40	982	206	217.8	238.4
14:00	43.5	58	49.5	1087	220.7	230.3	
14:15	46	59.7	50	1065	214.3	225.1	
14:30	48	62	53	1054	209.6	219.5	
14:45	52.5	66	44	1056	205.6	229.8	256.3
15:00	41.2	54.7	52.8	658	135.9	137.2	
15:15	42.7	54	53	879	182.1	183	
15:30	47.6	58	56	831	168.7	170.4	
15:45	45	58	43	810	164.4	177.1	196.6
16:00	44	56	51	705	144.6	148.3	

A section through Table 2 which, indicates the difference in the power output produced by the module when subjected to different conditions is as shown in Table 3

**Table 3.** Power outputs obtained from the experiment

Time	Module without Al heat sink power output (w) at f_{pv} = 95%	Module + Al heat sink & water-cooling, power output (w) at f_{pv} = 95%	Module + Al heat sink & water-cooling of module surface to 20°C power output (w) at f_{pv} = 95%
12:45	212.6	240.9	262.4
13:45	206	217.8	238.4
14:45	205.6	229.8	256.3
15:45	164.4	177.1	196.6

From Table 3 above, more power is obtained with the module + Al heat sink & water cooling, but maximum power output of 262.4 w was achieved with cooling the PV module + Al heat sink & water-cooling of module surface to 20°C.

In order to implement the effect of the increase in power output using MATLAB, the module operating temperature set to 20°C, is used as an input to the PV array MATLAB Simulink block.

4. Model composition of hybrid PV/wind/diesel generator

The research project comprises of 60kw PV array, 50kw diesel generator, 50kw PMSG driven wind turbine, 480 Vision 6FM200D batteries made up of a string size of 30 with 16 strings in parallel, each battery have a nominal voltage of 12volts and a nominal capacity of 200AH (2.4KWh). The configuration of the hybrid energy system is as shown in Figure 4
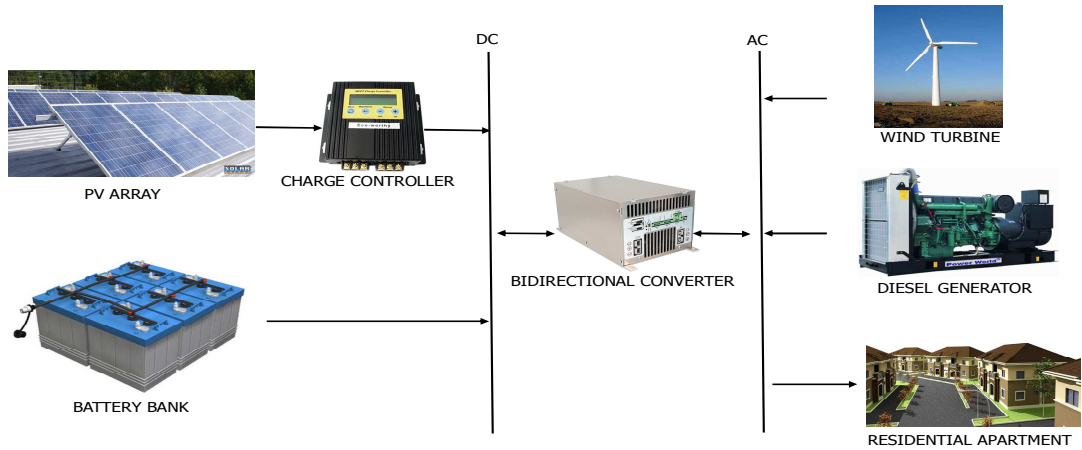
Figure 4. Hybrid energy system configuration

4.1. Design of 60kw PV array

The maximum power delivered by a photovoltaic array as in [5] is given by the expression

$$P_{mp} = (N_p \times I_{mp}).(N_s \times V_{mp}).$$ (4)

Where the N_p and N_s stand for the number PV modules connected in parallel and in series respectively. I_{mp} and V_{mp} stand for the maximum current and voltage at MPPT respectively. This is because adding PV modules in series increases the voltage while adding PV modules in parallel increases the current.

In order to achieve a PV array with a capacity of 60KW, a PV array voltage of 614V was considered by connecting 20 PV modules in series, conversely 12 PV modules are connected in parallel and each module has a maximum voltage, V_{mp} of 30.7v and a maximum current, I_{mp} of 8.15A at maximum power.

4.2. Sizing of battery bank

The size of the battery bank can be calculated as in [6] using equation (5).

$$B_{cp} = \frac{D_d.D_A}{\eta.V_{sys}.DoD}$$ (5)

Where DoD, η, V_{sys}, B_{cp}, D_d and D_A stand for depth of discharge, efficiency, Battery capacity, daily load demand and battery days of autonomy respectively. Battery round trip efficiency of 85% was selected for this project.

Sizing of battery bank for this project does not require any further design as the sizing was achieved with the help of HOMER software simulator. A total of 480 batteries, each with nominal voltage of 12V and a nominal capacity of 200Ah (2,4Kwh) is required for this project and it comprises of a string size of 30 with 16 battery strings in parallel.

Batteries add up in series to increase the voltage while the amperage remains the same, conversely, they add up in parallel to increase current while the voltage remains the same. A string size of 30 implies connecting 30 batteries in series.

This generates 30 (12V), at an amperage of 200Ah and hence, the bus voltage is 360V, hence a battery string size of 30 generates 360V, 200Ah. Sixteen, 16 parallel strings of battery connected in parallel yields 360V, 16 (200Ah). Therefore, the 480 batteries required for this research work generate a bus voltage of 360V and an amperage of 3200Ah.

4.3. Boost converter design

In this case, the boost converter is used to give the PV voltage, Vpv a boost from 614V to 700V, which is the selected V_{dc} of the VSC DC bus.

The boost converter duty cycle (D) is expressed as in [7] as

$$D = \left(\frac{V_{dc} - V_{pv}}{V_{dc}} \right) = \left(\frac{700 - 614}{614} \right) = 0.12 \tag{6}$$

The capacity of the boost converter inductor is given as

$$L_{bc} = \left(\frac{V_{in} D}{f_{sw} \Delta I_{pv}} \right) = \left(\frac{614 \times 0.12}{10 \times 10^3 \times \frac{5}{100} \left(\frac{60 \times 10^3}{614} \right)} \right) = 1.508\, mH \tag{7}$$

Where ΔI_{pv} is considered as the input current ripples (5%) of I_{pv} and f_{sw} represents the switching frequency in hertz, the value of the inductance, L_{bc} is selected as 1.6mH.

4.4. DC link capacitor design
The size of the DC link capacitor can be calculated as in [7] using the expression

$$C_1 = C_2 = \left(\frac{I_d}{2(2 \times \omega \times \Delta V_{dcrip})} \right) = \left(\frac{P / V_{dc}}{2(2 \times \omega \times \Delta V_{dcrip})} \right) = 4875\, \mu F \tag{8}$$

Where V_{dcrip} is the ripple voltage, its value is 2% of the V_{dc}, I_d represents the VSC DC link current, the angular frequency is represented by ω, the value of the selected DC link capacitors are C1=C2=500μF
Interfacing Inductor design and selection
The value of the interfacing inductor is achieved using the expression in [7] as

$$L_{int} = \left(\frac{\sqrt{3} \times m \times V_{dc}}{12 \times O_f \times f_{sw} \times I_{Rr}} \right) = \left(\frac{\sqrt{3} \times 0.90 \times 700}{12 \times 1.2 \times 900 \times 0.25 \times 86.60} \right) = 3.89\, mH \tag{9}$$

Where O_f represents the overloading factor, m represents the modulation index, fsw represents the switching frequency, Vdc represents the DC link voltage, I_{Rr} represents the ripple in the grid current, its value is 25% of the grid current, IR.

$$I_R = \left(\frac{60 \times 10^3}{\sqrt{3} \times 400} \right) = 86.60\, A \tag{10}$$

4.5. Modelling of diesel generator
The diesel generator is made up a diesel engine and an alternator for electricity generation; it consist of a diesel engine, a synchronous generator, an excitation system and speed controller. The diesel engine and governor system exert control on the speed of the governor to supply mechanical power. Its diesel engine comprises of the governor and an internal combustion (IC) engine.
The diesel generator ensures the conversion of energy from fuel such as diesel or bio-diesel into mechanical energy with the help of its internal combustion engine, after which, this mechanical energy is converted into electrical energy with the help of its electric machine operating as a generator. The governor is made up of actuator and speed controller, the maintenance of a constant speed during the period of operation of a diesel generator is maintained by the governor [8] [9]
The transfer function of the actuator as well as that of the regulator as in [8] is as shown in equation 11 and 12 respectively

$$H_a = \frac{(1 + T_{a1} s)}{s (1 + T_{a2} s) + (1 + T_{a3} s)} \tag{11}$$

$$H_r = \frac{\Upsilon_r (1 + T_{ra} s)}{(1 + T_{r1} s + T_{r2} s^2)} \tag{12}$$

Where, T_{a1}, T_{a2} and T_{a3} represent the time constants of the actuator, Υ_r represents the gain of the regulator while, the time constants of the regulator is represented by T_{r1}, T_{r2} and T_{r3}.
Conversely, the speed regulation and diesel engine of the diesel generator can be described using differential equations as in [8] as equation (13) and equation (14).

$$\frac{dm_B}{dt} = \frac{1}{\tau_2} (K_2 P_c - \frac{K_2}{\omega_{ref} R} \Delta \omega - m_B) \tag{13}$$

$$\frac{dP_c}{dt} = \frac{-K1}{\omega_{ref}} \Delta \omega \tag{14}$$

Where the rate of fuel consumption of the diesel engine is denoted m_B, ω_{ref} is the engine reference speed in rad/sec, R is the permanent speed drop of the diesel engine, K_1 is the summing loop amplification factor of the governor, the gain and dead time of the engine is represented by K_2 and Υ_2 respectively. The dead time, Υ_2 can be represented as in [8] as equation (15).

$$\tau_2 = \frac{60 S_t}{2 N n} + \frac{60}{4 N} \tag{15}$$

N refers to the speed in rev/min, n is the quantity of cylinders, S_t represents the number of stroke engine, in this case, $S_t=4$ and due to combustion, the generated mechanical power is expressed as equation (16)

$$P = E_1 m_B \eta \tag{16}$$

η represents the efficiency and E_1 represents the proportionality constant.

4.6. Modelling of wind energy conversion system

With the help of the wind turbine, wind energy is converted into mechanical power and hence. The mechanical power is transformed into electrical power. The value of the mechanical power can be computed using the equation (17) [10]

$$P_m = 0.5 \rho A C_p(\lambda, \beta) V_{wind} \tag{17}$$

Where ρ represents the density of air, its value is within the range of 1.22-1.3Kg/ms, V_{wind} refers to the speed of the wind in m/s, A represents the swept area of the turbine blades (m^2), the coefficient of power is denoted by $C_p(\lambda,\beta)$, it's influenced by two factors, the pitch angle of the blade, β and the speed slip ratio, mathematically, the tip speed ratio is defined as

$$\lambda = \Omega R / V_{wind} \tag{18}$$

R is the radius of the blade (m) and Ω refers to the angular speed (m/s)

The coefficient of power is defined as in [10] as

$$C_p(\lambda, \beta) = C_1 \left(\frac{C_2}{\lambda_1} - C_3 \beta - C_4 \right) \exp\left(\frac{-C_5}{\lambda_1} \right) + C_6 \lambda \tag{19}$$

Where

$$\frac{1}{\lambda 1} = \left(\frac{1}{\lambda + 0.08\beta} - \frac{0.035}{\beta^3 + 1} \right) \tag{20}$$

The rotational torque can be expressed as

$$T_m = P_m / \Omega \tag{21}$$

And the optimal angular speed is represented by the relation

$$\Omega opt = \lambda_{opt} V_{wind} / R \tag{22}$$

In order to achieve the maximum mechanical power, the following relation is used

$$P_{m\_max} = 0.5 \rho A C_{p\,max} V^3_{wind} \tag{23}$$

4.6.1. PMSG driven wind turbine

The PMSG driven wind turbine was chosen for this project as a result of certain advantages in [11] as follows:
- There are absence of brush/slip ring.
- The mechanical stress is low
- The rotor does not experience any form of copper loss
- Reactive/active power controllability is higher

The sign of the torque input of the PMSG is what determines its mode of operation, if its sign is negative, the PMSG operates as a generator and if its sign is positive, the PMSG operates as a motor [12].

The implementation of PMSG model is done in the dq-coordinates, which implies AC states does not exist in the model. Its mathematical equation is developed from the synchronous rotating reference frame by ensuring that the d-axis aligns with the rotor flux direction [10] [13].

$$V_q = R_s i_q + L_q \frac{di_q}{dt} - \omega_e L_d i_d + \omega_e \varphi_m \tag{24}$$

$$V_d = R_s i_a + L_d \frac{di_a}{dt} - \omega_e L_q i_q \tag{25}$$

Where V_q and V_d represent the q and d components of the voltages in the stator, i_q and i_d represent the q and d components of the currents in the stator, L_q and L_d represent the inductances (H) of the machine, φ_m represents the magnetic flux (wb), ω_e represents the electrical speed (rad/s).

In order to obtain the electrical torque, the following expression is used.

$$Te = \frac{3}{2} P \left\{ \varphi_m i_q + \left(L_d - L_q \right) L_d i_q \right\} \tag{26}$$

P in the expression above represents the poles pair and the machine rotor dynamics can be represented by the following expression

$$T_m - T_e = B\omega_r + J \frac{d\omega_r}{dt} \tag{27}$$

Where J represents the inertia of the rotor (kgm^2), ω_r is the speed of the rotor (rad/s), B represents the friction in the rotor Kgm^2/s, the mechanical torque that was produced by the wind is represented by T_m Assuming $L_d=L_q=0$, and the d-reference current, $id^*=0$, then the $(L_d-L_q)i_d i_q$ becomes negligible.

4.7. Control of the hybrid energy system

The battery bank performs two roles in this project as it serves a sink, and also as a source, hence it charges or discharges when the network experiences surplus or lack of power from the sources of energy due to the situation of the weather. When the amount of electricity supplied by the sources of power is greater the load on the network, the battery controller charges the battery and when the load on the network is more than the electricity supply from the sources, the controller causes the battery bank to discharge [14].

The control of the battery storage is done in such a way as to ensure the DC voltage is stabilized and this is achieved through the control of the DC/DC bidirectional converter in the network.

When there is a shortage of power from the sources, the bidirectional converter serves as a boost converter to provide power by discharging the battery and when the power supplied from the sources is in excess, it operates as a buck converter to charge the battery [15].

The hybrid system is also, incorporated with a dump load, the dump load is made up of a bank of resistors and a power converter, the capacity of the dump load power is such that it exceeds the amount of power produced by the wind, PV and diesel generator by 30%. It is to ensure the control of the network should, a condition arises when there is no load and the battery storage fails or is fully charged.

The flow of power in the network can be represented as

$$P_{network} = P_{pv} + P_{wt} + P_{diesel} - P_{load} \tag{28}$$

Where, the net power generated is represented by $P_{network}$, P_{pv} is the amount of power supplied by the PV, P_{wt} represents the power supplied by the wind turbine and P_{load} is the power of the load

When $P_{network} < 0$, it means the power supplied by the energy sources is not enough and the battery provides power to make up for the shortage of power, but when $P_{network} > 0$, it implies the amount of power produced by the energy sources is in excess, the excess power is stored in the battery, but the moment it becomes more than the rated power of the batteries in the battery bank, a fraction of the excess power is transferred to the system dump load.

5. Results

The results obtained from the simulations carried out from the project implementation using MATLAB Simulink are as shown in Figure 5.
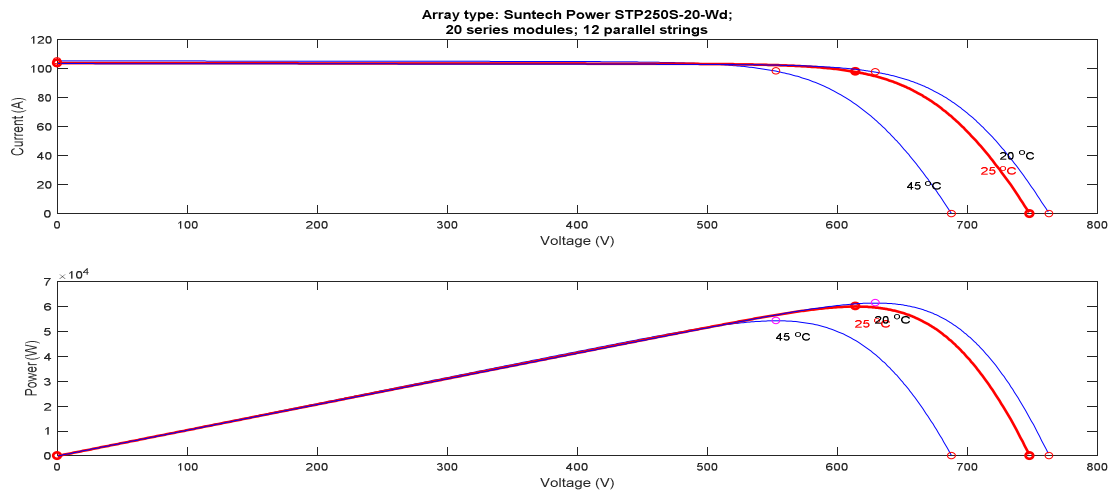
Figure 5. I-V and P-V curve of 60KW PV array.

The I-V and P-V curve below shows the usual characteristic of a PV module, which generate less power as the temperature of the module increases.

The research location for this project usually experiences low wind speed unlike some part of Europe where the wind speed is high and as a result the simulation was carried out at a wind speed of 6.1m/s and at a constant irradiance of 1000w/m². The result is as shown in Figure 6 and Figure 7.
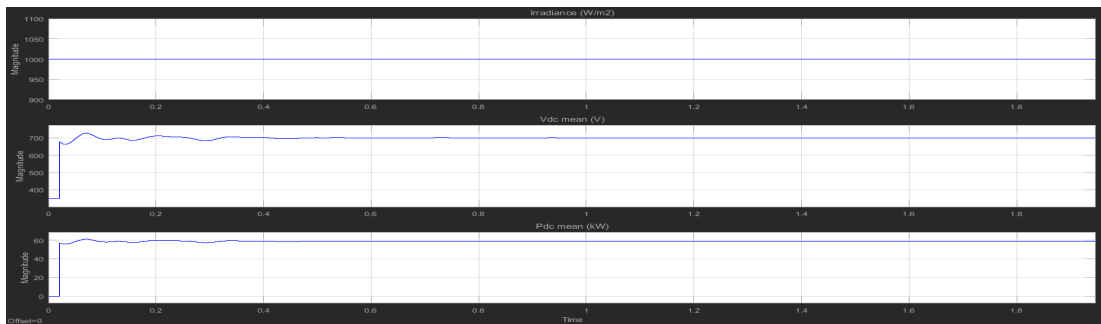

Figure 6. 60KW PV array power output at 45°C.
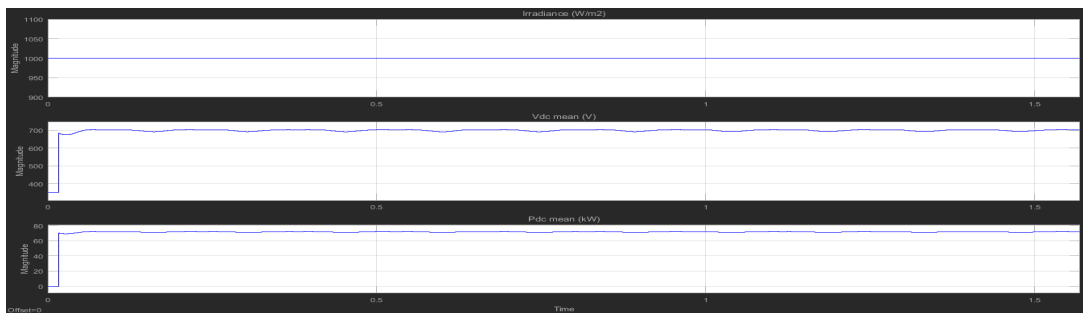
Figure 7. 60KW PV array power output at 20°C.

From Figure 6 and Figure 7, it can be observed that the power output produced by the PV array at a temperature of 20°C is more, this is because, the PV module works better when the module surface temperature is low

The measured Vdc and the reference Vdc of the network were compared and the values obtained are very close as shown in Figure 8
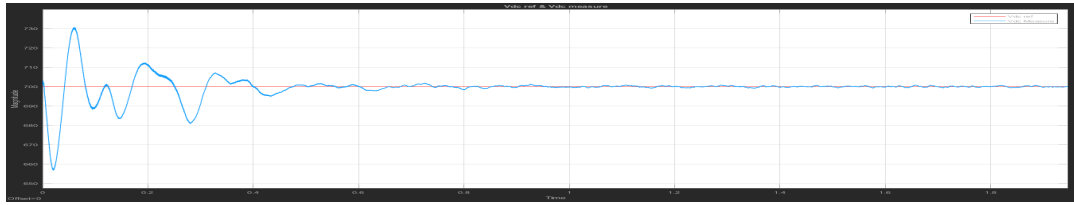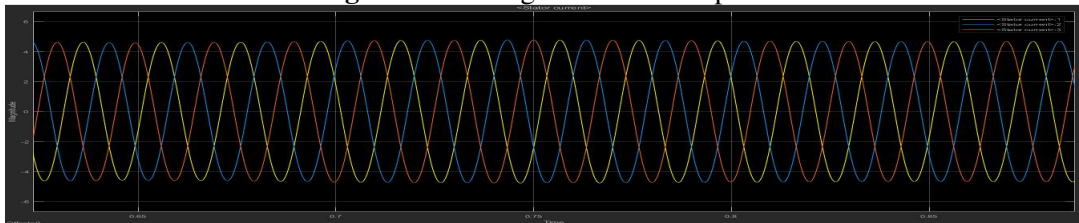
Figure 8. Vdc reference and Vdc measured

The diesel generator rotor speed in pu and the stator currents are as shown in Figure 9 and Figure 10 respectively
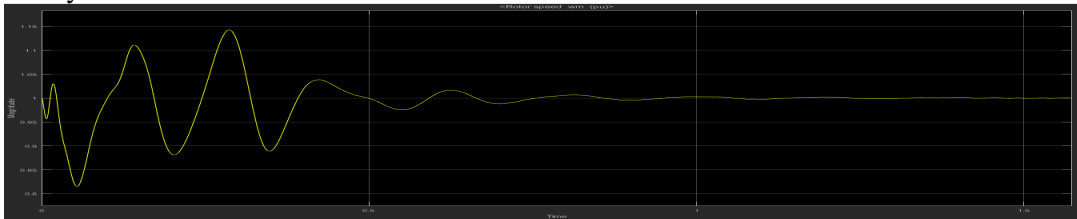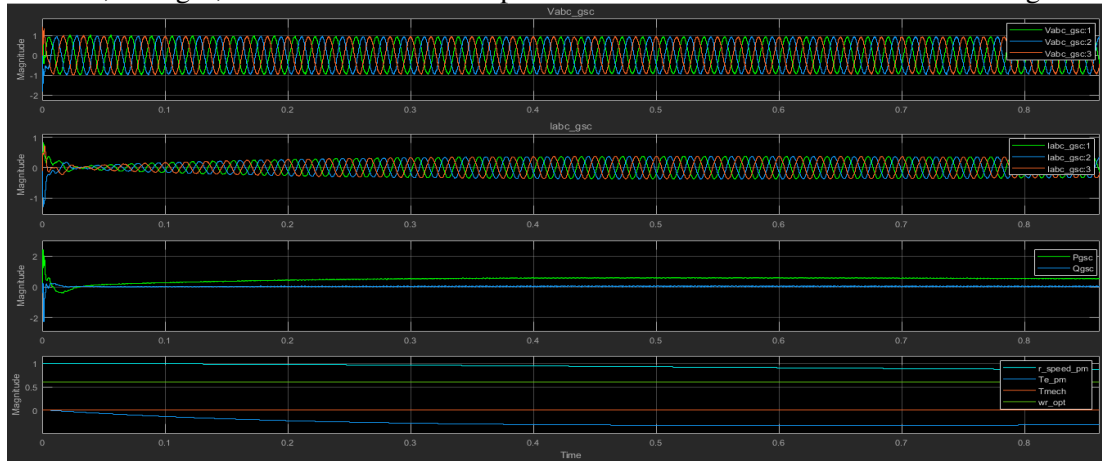

Figure 9. Diesel generator rotor speed.

Figure 10. Diesel generator stator currents

The currents, voltages, the active and reactive power of the wind turbine are as shown in Figure 11.

Figure 11. Wind turbine currents, voltages, active and reactive power output

6. Conclusion

The reduction in the surface temperature of the PV module increases the efficiency of the PV module, this results in an increase in the power output obtained from the experiment. The experiment shows that an increase in power output from 250watts to 262.4 watts is achievable. The result of the simulation also shows that at a temperature of 20°C, the PV module contributes more power to the hybrid energy system than at a temperature of 45°C. Hence, there is an increase in the hybrid PV/Wind/Diesel generator power output with increased module efficiency. Future works in this project involve the provision of voltage control of the hybrid energy system.

7. References

[1] Engin M. Sizing and simulation of PV-wind hybrid power system. Int J Photoenergy. 2013;2013

[2] Chikate B V, Sadawarte Y A. The Factors Affecting the Performance of Solar Cell. Int J Comput Appl Sci Technol [Internet]. 2015 [cited 2017 Sep 16];975–8887. Available from: http://research.ijcaonline.org/icquest2015/number1/icquest2776.pdf

[3] Koteswararao B, Radha K, Vijay P and Raja N. Experimental Analysis of solar panel efficiency with different modes of cooling. 2016;8(3):1451–6.

[4] Homer Energy. How homer calculates the PV array power output [Internet]. Homer Energy Support. 2014 [cited 2017 Oct 31]. p. 1. Available from: https://www.homerenergy.com/support/docs/3.10/how_homer_calculates_the_pv_array_power_output.html

[5] Kumar S, Verma A K, Hussain I and Singh B. Performance of Grid Interfaced Solar PV System under Variable Solar Intensity. [cited 2017 Nov 22]; Available from: https://www.researchgate.net/profile/Ikhlaq_Hussain/publication/280562137_Performance_of_grid_interfaced_solar_PV_system_under_variable_solar_intensity/links/55b9c8c608aed621de0879dc/Performance-of-grid-interfaced-solar-PV-system-under-variable-solar-inte

[6] Akinyele D O and Rayudu R K. Community-based hybrid electricity supply system: A practical and comparative approach. Appl Energy [Internet]. Elsevier Ltd; 2016;171:608–28. Available from: http://dx.doi.org/10.1016/j.apenergy.2016.03.031

[7] Mohan N, Undeland T M and Robbins W P. Power electronics : converters, applications, and design. 3rd ed. John Wiley & Sons; 2003. 824 p.

[8] Faten Hosney Fahmy. PV/Diesel Hybrid System for Fuel Production from Waste Plastics Recycling. Ijmer [Internet]. 2014;4(12):68–79. Available from: http://www.ijmer.com/papers/Vol4_Issue11/Version-1/H04011_01-6879.pdf

[9] Pachori A, Suhane P and Scholar P. Design and modelling of standalone hybrid power system with MATLAB/simulink. Int J Sci Res Manag Stud [Internet]. [cited 2017 Dec 3];1(2):2349–3771. Available from: http://www.ijsrms.com/media/3n2-IJSRMS0102116_v1_is2_65-71.pdf

[10] Babu N R and Arulmozhivarman P. Wind energy conversion systems - A technical review. J Eng Sci Technol. 2013;8(4):493–507.

[11] Kim H S and Lu D D. Wind Energy Conversion System from Electrical Perspective — A Survey. 2010;2010(November):119–31. Available from: http://www.scirp.org/journal/PaperInformation.aspx?PaperID=3324

[12] Mishra S, Gupta M, Garg A, Goel R and Mishra V K. Modeling and Simulation of Solar Photo-Voltaic and PMSG Based Wind Hybrid System. lEEE Students' Conference on Electrical, Electronics and Computer Science [Internet]. 2014 [cited 2017 Nov 19]. Available from: http://ieeexplore.ieee.org/stamp/stamp.jsp?arnumber=6804430

[13] Gajewski P and Pieńkowski K. Analysis of a wind energy converter system with PMSG generator. 2015;

[14] Samrat N H, Ahmad N Bin, Choudhury I A and Taha Z B. Modeling , Control , and Simulation of Battery Storage Photovoltaic-Wave Energy Hybrid Renewable Power Generation Systems for Island Electrification in Malaysia Modeling , Control , and Simulation of Battery Storage Photovoltaic-Wave Energy Hybrid Renewab. Sci World J. 2014;2014(February 2016):22.

[15] Yasin A, Napoli G, Ferraro M and Antonucci V. Modelling and control of a residential wind/PV/battery hybrid power system with performance analysis. J Appl Sci [Internet]. 2011 [cited 2017 Sep 6];11(22):3663–76. Available from: http://www.scialert.net/qredirect.php?doi=jas.2011.3663.3676&linkid=pdf